Optical Materials 72 (2017) 513–517

Contents lists available at ScienceDirect

Optical Materials

journal homepage: www.elsevier.com/locate/optmat

Optical nonlinearity, limiting and switching characteristics of novel ruthenium metal-organic complex

K.B. Manjunatha [a, *], Ravindra Rajarao [b], G. Umesh [c], B. Ramachandra Bhat [d], P. Poornesh [e]

[a] Department of Physics, NMAM Institute of Technology, Nitte 574110, India
[b] Centre for Sustainable Materials Research and Technology, School of Materials Science and Engineering, University of New South Wales, Sydney, NSW 2052, Australia
[c] Optoelectronics Laboratory, Department of Physics, National Institute of Technology Karnataka, Mangalore 575025, India
[d] Catalysis and Materials Laboratory, Department of Chemistry, National Institute of Technology Karnataka, Mangalore 575025, India
[e] Nonlinear Optics Research Laboratory, Department of Physics, Manipal Institute of Technology, Manipal University, Manipal 576 104, Karnataka, India

ARTICLE INFO

Article history:
Received 16 March 2017
Received in revised form
24 May 2017
Accepted 27 June 2017
Available online 1 July 2017

Keywords:
Nonlinear optics
Z-scan
DFWM
Optical limiting

ABSTRACT

We report the nonlinear optical properties of Ruthenium metal complex a promising organic material for use in scientific and technological applications. The thin films of newly synthesized ruthenium metal −organic complex were fabricated using spin coating technique. Z-scan and degenerate four wave mixing (DFWM) techniques used to extract the third-order nonlinear optical (NLO) parameters. The data reveals the investigated material exhibited relatively large NLO properties. The pump−probe experiments shows that the switch-on and off times of the material were in the order of μs at different pump intensities and the energy dependent transmission studies reveal good limiting property of the material in nanosecond regime.

1. Introduction

Metal-organic or organometallic materials have received significant interest over the past decade because of their large NLO properties and have possible applications in optical devices such as all-optical switching, power limiters etc [1–4]. High nonlinearity, ease in structural modifications, relatively cheap and ease in synthesis make these materials more attractive and have the capability of replacing the inorganic systems [5]. Organometallic systems obtained by the incorporation of transition metal ions into organic systems, which introduces more sublevels into the energy hierarchy, thus permitting more allowed electronic transitions and resulting in larger NLO effects. The advantages of organometallic systems are by changing metal ion and/or surrounding organic environment we can tune the NLO properties [5–7].

Keeping this in mind, we synthesized new salophene based ruthenium complex and investigated the NLO properties using Z-scan and DFWM technique. To explore the suitability of the material for photonic device applications, all-optical switching and optical power limiting measurements were carried out using pump-probe and energy dependent transmission techniques respectively.

2. Experimental techniques

2.1. Materials and methods

Analytical grade chemicals were used. Solvents were purified and dried according to standard procedure (Vogel 1989). Ruthenium (III) chloride trihydrate and all other reagents were procured from Sigma Aldrich Chemicals, and were used without further purification. The synthesis of ligand, salophene (L) = *N*, *N*′-disalicylidene-1,2-ethylendiimine dianion is reported in elsewhere [8].

The Ru(II) Schiff base complex, Ru (salophene) (H_2O) (Cl) (named as Ru-L) was prepared in high yield via the interaction of the free Schiff base, H_2L, with $RuCl_3.3H_2O$ in a 1:1 mol ratio in refluxing absolute ethanol for 12 h. Ru-L: 1H NMR (DMSO-d_6): δ 8.40 (s, 2H, *HC*=N), 7.88–7.86 (m, 2H, Ar*H*), 7.37–7.34 (m, 2H, Ar*H*), 7.03 (d, *J* 7.6 Hz, 2H, Ar*H*), 6.86 (d, *J* 7.6 Hz, 2H, Ar*H*) and 6.44 (t, *J* 7.6 Hz, 2H, Ar*H*). IR (cm-1, KBr): 3314 m, 1613 s, 1585 s, 1540 s,

* Corresponding author.
E-mail addresses: manjukb15@nitte.edu.in (K.B. Manjunatha), poorneshp@gmail.com (P. Poornesh).

http://dx.doi.org/10.1016/j.optmat.2017.06.051
0925-3467/

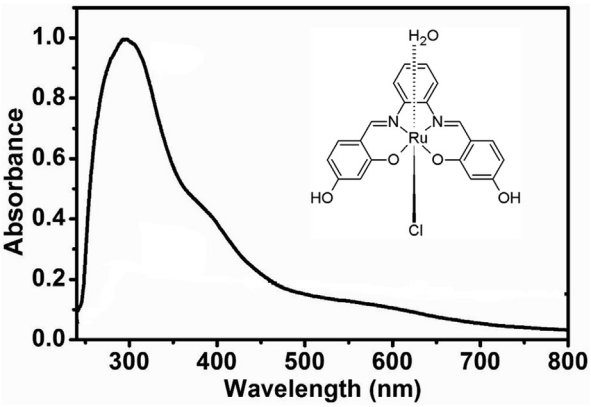

Fig. 1. UV–visible absorption spectrum of the sample Ru-L. Inset Molecular Structure of Ru-L.

1467 s, 1444 s, 1389 m, 1238 s, 1193 s, 1107 m, 975 m, 737 s.

NLO properties were investigated in both liquid and solid form. Liquid samples of different concentrations were obtained by dissolving material into *N*,*N*-dimethylformamide (DMF). Solid samples of different concentrations were fabricated using spin coating technique [9]. The Z-scan and DFWM techniques were used to determine the NLO properties of the samples [10–16]. Optical power limiting studies of the samples carried out by energy dependent transmission technique [9]. All-optical switching characteristics were performed using standard pump-probe technique [9,16].

3. Results and discussion

The molecular structure and UV–Vis absorption spectra of the sample are shown in Fig. 1. The peaks between 230 and 350 nm are attributed to intra-ligand charge transfer transitions and small peak in between 390 and 500 nm represents the DMSO-d_6 forbidden transitions.

3.1. Z-scan studies

The open aperture Z-scan technique was used obtain the magnitude and sign of nonlinear absorption (NLA) coefficient (β_{eff}) of the sample. Fig. 2 shows the open aperture Z-scan curves of the sample with theoretical fits [10,17] and characteristics of the curve suggests the intensity dependent absorption of the sample. Reverse saturable absorption (RSA) via excited state absorption (ESA) is attributed for large NLA in the sample, this can be explained with five-level model reported in the literature [17]. The excited state absorption cross section σ_{exc}, can be measured using the normalized energy transmission of open aperture Z-scan [18–21].

$$T = \ln\left(1 + \frac{q_0}{1+x^2}\right) \Big/ \left(\frac{q_0}{1+x^2}\right), \tag{1}$$

where $q_0 = \frac{\sigma_{exc}\alpha F_0(r=0)L_{eff}}{2\hbar\omega}$,

$X = z/z_o$, z is the distance of the sample from the focus, z_o is the Rayleigh length given by the formula $Z_o = k\omega_0^2/2$, where k is the wave vector and ω_o is the beam waist at the focus$L_{eff} = [1 - \exp(-\alpha L)]/\alpha$, and F_o is the on -axis fluence at the focus.

The value of excited state absorption cross section σ_{exc}, were obtained by fitting the open aperture data using equation (1) and the ground state absorption cross section, σ_g, were calculated using the relation given below and the values are given in Table 1,

$$\alpha = \sigma_g N_a C, \tag{2}$$

where N_a is the Avogadro's number and C is the concentration in mol/L.

The magnitude of ESA cross-section, σ_{exc} larger than ground-state absorption cross-section, σ_g of the sample suggests that the NLA is due to RSA. In Fig. 3, the value of β_{eff} decreases while increasing the on-axis intensity I_0 which is evident of NLA due to RSA [22]. The closed aperture Z-scan technique was used to obtain the pure nonlinear refraction. Fig. 4 shows the pure nonlinear refraction Z-scan curves with theoretical fits of the sample. The signature of the curve indicates the nonlinear refractive index (n_2) is negative (self-defocusing effect). The magnitude of n_2 and $\mathrm{Re}\chi^{(3)}$ were determined and tabulated in Table 1. The thermal effects were taken in to account in the experiments by performing in the single shot mode. More over the closed aperture z-scan curve displays a peak-valley separation of less than ~1.7Z_R. A peak-valley separation of more than 1.7 times the Rayleigh range (Z_R) is the signature of thermally induced nonlinearity and hence thermal effects can be neglected. Hence, the observed nonlinearity is predominantly electronic in nature, in addition there is a possible presence of orientational contribution to the observed nonlinearity [23].

3.2. DFWM studies

The magnitude of $\chi^{(3)}$ was also determined using DFWM technique. The variation of DFWM signal with pump energy of CS_2 and sample are shown in Fig. 5 where the solid line is the cubic fit to the experimental data. The $\chi^{(3)}$ data of the sample was obtained by comparing the DFWM signal of CS_2 and calculated using the following equation [24],

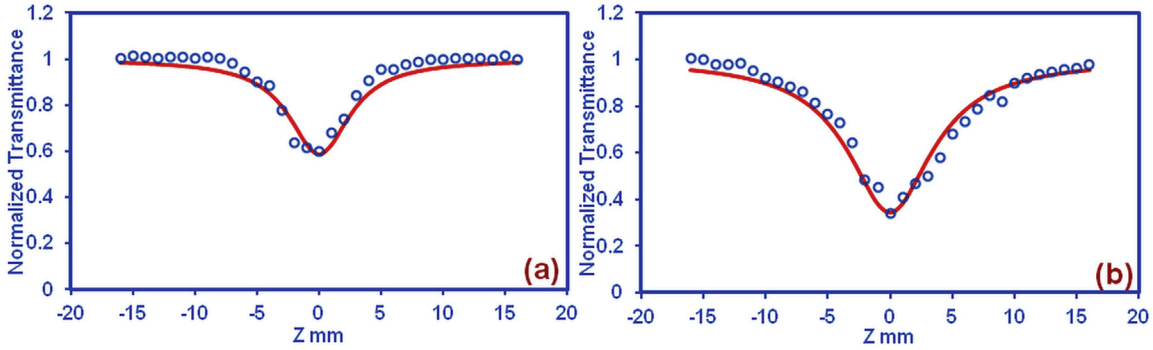

Fig. 2. Open aperture Z-scan of (a) sample in liquid form at the concentration of 2.5 × 10^{-4} mol/L and (b) sample in solid form at the concentration of 0.5 wt%. In (a) and (b) solid line depicts theoretical fit.

Table 1
Third-order nonlinear optical parameters of the sample in liquid form.

Concentrations (x 10^{-4} mol/L)	β_{eff} (m/W) × 10^{-11}	Im $\chi^{(3)}$ (esu) × 10^{-13}	σ_g (cm^2) × 10^{-19}	σ_{exc} (cm^2) × 10^{-18}	N_2 (esu) × 10^{-11}	Re $\chi^{(3)}$ (esu) × 10^{-13}
2.5	11.574	1.741	8.827	3.626	−5.895	−6.221
5	17.052	2.565	5.698	4.683	−7.503	−7.918
10	32.648	4.912	5.442	5.824	−13.852	−14.618

Table 2
Third-order nonlinear optical parameters of the sample in solid form.

Dopant concentration (Wt%)	β_{eff} (m/W) × 10^{-9}	Im $\chi^{(3)}$ (esu) × 10^{-11}	σ_g (cm^2) × 10^{-17}	σ_{exc} (cm^2) × 10^{-16}	n_2 (esu) × 10^{-9}	Re $\chi^{(3)}$ (esu) × 10^{-10}
0.50	20.778	4.574	9.643	4.742	−11.408	−1.551
1.00	25.103	5.526	6.393	5.729	−13.727	−1.867
1.50	27.003	5.944	5.759	6.162	−14.856	−2.020
2.00	38.884	8.560	4.978	8.874	−20.324	−2.764

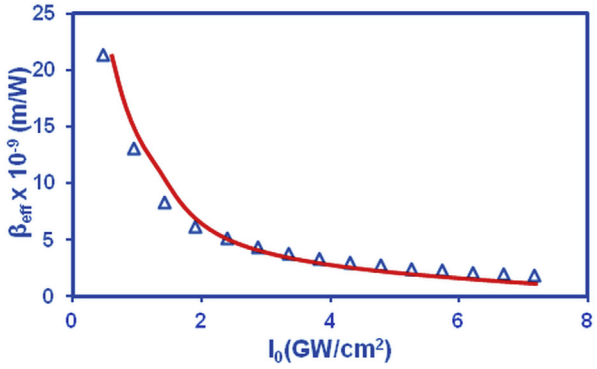

Fig. 3. Nonlinear absorption coefficient (β_{eff}) vs. on-axis input intensity I_0 of the sample.

$$\chi^{(3)}_{sample} = \chi^{(3)}_{ref}\left(\frac{I_{sample}}{I_{ref}}\right)^{1/2}\left(\frac{n_{sample}}{n_{ref}}\right)^{2}\left(\frac{l_{ref}}{l_{sample}}\right) \times \left(\frac{\alpha l}{e^{-\alpha l/2}(1-e^{-\alpha l})}\right)$$

where *I*, *n*, *l* and α are the DFWM signal intensity, refractive index, length of the medium and linear absorption-coefficient respectively. The 'ref' refers to CS_2, the $\chi^{(3)}_{ref}$ is taken to be 4×10^{-13} esu [25] and estimated $\chi^{(3)}$ value of the complex is 1.486×10^{-12} esu. The values of third order nonlinear optical susceptibility $\chi^{(3)}$ obtained by the DFWM technique were consistent with the values obtained by the single beam Z-scan technique.

Results show that NLO properties of sample in solid form possess two orders of magnitude larger than that in sample in liquid form. This is due to the number molecules in solid form is more than that in the liquid form, which creates large number of absorbing centers [26].

The $\chi^{(3)}$ values of the investigated complex are one order larger compare to the values obtained for thin films of metallophthalocyanine chlorides by A. Zawadzka et al. [27] and for porphyrin nanorods obtained by N. Mongwaketsi [28]. The obtained values were also comparable with metallophthalocyanines (MPcs, with M = Co, Cu, Zn, Mg) thin films obtained by B. Derkowska [29], ruthenium and iron metal complexes obtained by K. Iliopoulos et al. [30], bis-iminopyridine-tetrathiafulvalene appended ligand obtained by K. Iliopoulos et al. [31] and also comparable with values obtained for Azo-Based Iminopyridine Ligand by Imen Guezguez [32]. The values of the complex were also two orders less compared to the values obtained for metallophthalocyanine thin films nanostructures obtained by A. Zawadzka et al. [33].

The linear and nonlinear optical properties of the Ru (II) complex with salophene ligand investigated here is a combination of aliphatic and aromatic diimine bridges. The N_2O_2 tetradentate ligand with delocalized π-systems impart strong ligand fields leading to almost square-planar geometries and low-spin ground states for the metal complexes (for those that have more than one spin ground state), inducing high degrees of covalence/delocalization within the metal–ligand bonds. The presences of these electronic properties are important in the design of molecules with high nonlinear optical properties. NLO responses can also be fine tuned by the extending π-conjugation through metal [34,35].

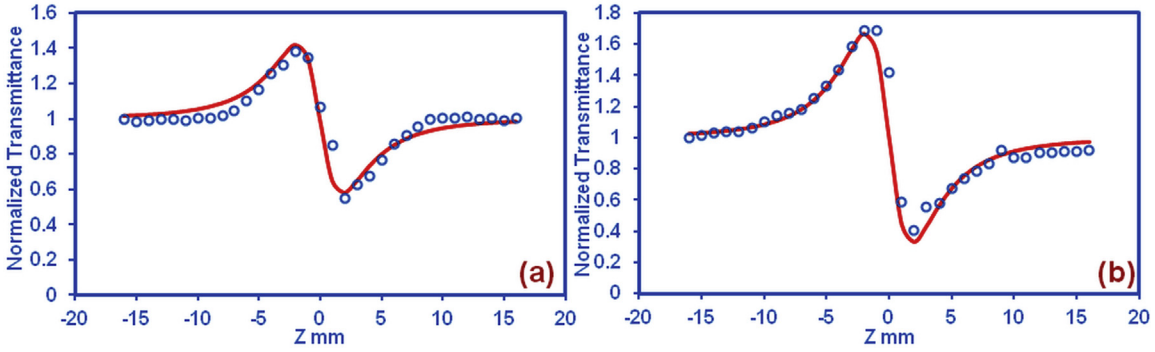

Fig. 4. Pure nonlinear refraction Z-scan of (a) sample in liquid form at the concentration of 2.5×10^{-4} mol/L and (b) sample in solid form at the concentration of 0.5 wt%. Solid line depicts theoretical fit.

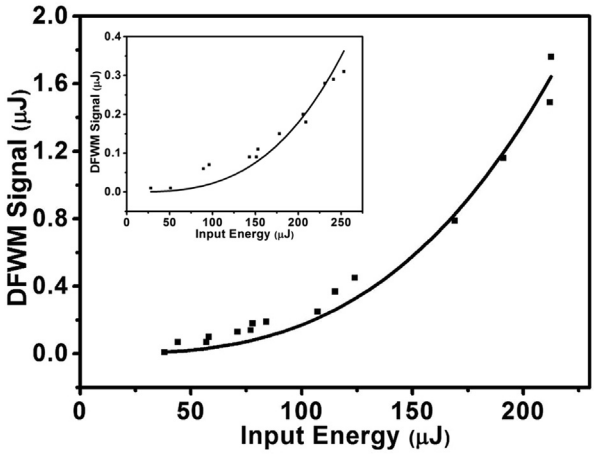

Fig. 5. DFWM signal of sample in liquid form at concentration of 1×10^{-3} mol/L. Inset shows DFWM signal of CS_2.

3.3. Optical power limiting studies

The large NLA in the sample leads to exhibit good power limiting property is shown in Fig. 6. The output energies are clamped at ~34, ~24 and ~18 μJ at the concentrations of 2.5×10^{-4}, 5×10^{-4} and 10×10^{-4} mol/L respectively for sample in liquid form and for sample in solid form the output energies are clamped at ~52, ~41, ~32 and 26 μJ at the concentrations of 0.5, 1.0, 1.5 and 2.0% respectively. Thus, investigated sample would be a promising material for making optical power limiting devices.

3.4. All-optical switching (AOS) studies

The all-optical switching behaviour of the sample is shown in Fig. 7. The modulation of the probe was observed to be 23, 29 and 38% for pump-beam intensities of 5, 10 and 15 GW/cm^2, respectively. The higher probe modulation at higher intensity of pump beam may be ascribed to the increase in the population of triplet state [36]. The switching response times were in the range of a few micro seconds. The relaxation of the triplet state to the ground state is forbidden, resulting in slow switching time of the molecules [37]. In fact, the observed optical switching indicates that one can fabricate an optical inverter or NOT gate.

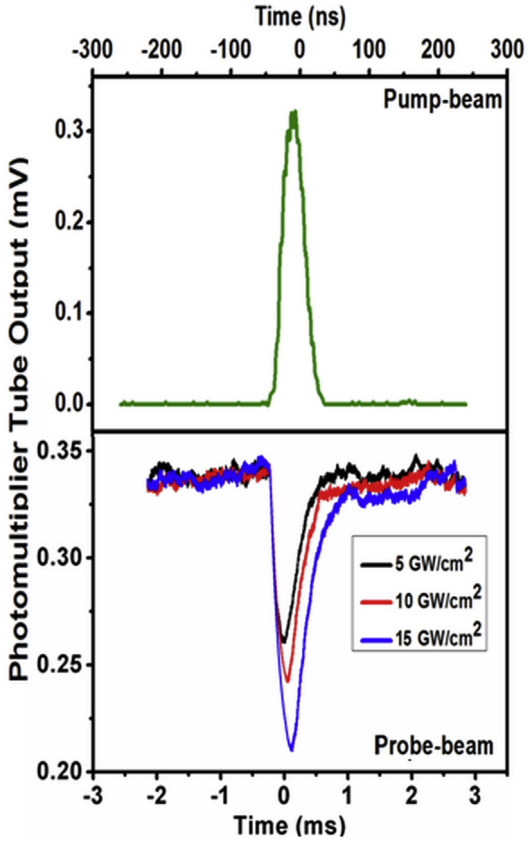

Fig. 7. All-optical switching response of the sample with various pump intensities.

4. Conclusions

In summary, the third-order nonlinear optical parameters of the complex were extracted and compared using the Z-scan and DFWM techniques at 532 nm with 7 ns pulses. The Z-scan results shows that the complex exhibits negative nonlinear refractive index and reverse saturable absorption. The value of excited state absorption cross-section, σ_{exc} of the complex is larger than ground-state absorption cross-section, σ_g suggests that the nonlinear absorption occurs mainly due to RSA assisted process. The real and imaginary parts of third-order nonlinear optical susceptibility $\chi^{(3)}$ were of the order of 10^{-11} esu which is comparable to the well NLO materials belonging to the class of organometallics. The observed nonlinearity is predominantly electronic in nature, in addition to the possible presence of orientational contribution to the nonlinearity. The complex investigated here possess good optical power limiting capability based reverse saturable absorption process indicating the photo thermal stability of the complex which is essential for use in protecting human eye and optical detectors. All-

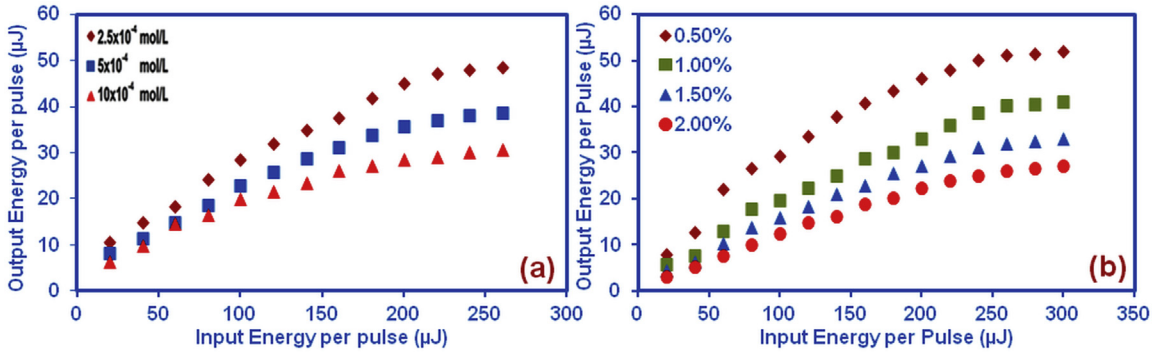

Fig. 6. Optical power limiting response of (a) sample in liquid form and (b) sample in solid form at various concentrations.

optical switching performance indicates that the material can be used to fabricate an optical inverter, hence the complex investigated here is a potential material for fabricating optoelectronics devices.

References

[1] Beibei Gao, Leszek M. Mazur, Mahbod Morshedi, Adam Barlow, Huan Wang, Cristóbal Quintana, Chi Zhang, Marek Samoc, Marie P. Cifuentes, Mark G. Humphrey, Chem. Commun. 52 (2016) 8301.
[2] C. Yadav, S. Roy, Opt. Quant. Electron. 49 (2017) 25.
[3] D. Wei, M.S. Kodikara, M. Morshedi, G.J. Moxey, H. Wang, G. Wang, C. Quintana, C. Zhang, R. Stranger, M.P. Cifuentes, M.G. Humphrey, ChemPlusChem 81 (2016) 621.
[4] K.B. Manjunatha, R. Dileep, G. Umesh, M.N. Satyanarayan, B. Ramachandra Bhat, Opt. Mater. 36 (2014) 1054.
[5] T. Huang, Z. Hao, H. Gong, Z. Liu, S. Xiao, S. Li, Y. Zhai, S. You, Q. Wang, J. Qin, Chem. Phys. Lett. 451 (2008) 213.
[6] H. Chao, R.H. Li, B.H. Ye, H. Li, X.L. Feng, J.W. Cai, J.Y. Zhou, L.N. Ji, Chem. Soc. Dalton Trans. 21 (1999) 3711.
[7] A. Migalska-Zalas, Z. Sofiani, B. Sahraoui, I.V. Kityk, S. Tkaczyk, V. Yuvshenko, J.-L. Fillaut, J. Perruchon, T.J.J. Muller, J. Phys. Chem. B 108 (2004) 14942–14947.
[8] M. Amirnasr, K.J. Schenk, A. Gorji, R. Vafazadeh, Polyhedron 20 (2001) 695.
[9] K.B. Manjunatha, R. Dileep, G. Umesh, B. Ramachandra Bhat, Opt. Mater. 36 (2013) 1366.
[10] M.S. Bahae, A.A. Said, T.H. Wei, D.J. Hagan, E.W. Van Stryland, IEEE J. Quant. Electron. 26 (1990) 760.
[11] K. Iliopoulos, A. El-Ghayoury, B. Derkowska, A. Ranganathan, P. Batail, D. Gindre, B. Sahraoui, Appl. Phys. Lett. 101 (2012) 261105.
[12] J.M. Hales, J.W. Perry, in: S.-S. Sun, L.R. Dalton (Eds.), Introduction to Organic Electronic and Optoelectronic Materials and Devices, CRC Press, Boca Raton, FL, 2008.
[13] K.B. Manjunatha, R. Dileep, G. Umesh, B. Ramachandra Bhat, Opt. Laser Technol. 52 (2013) 103.
[14] K.B. Manjunatha, R. Dileep, G. Umesh, B. Ramachandra Bhat, Opt. Laser Technol. 52 (2013) 103.
[15] K.B. Manjunatha, R. Dileep, G. Umesh, B. Ramachandra Bhat, Mat. Lett. 105 (2013) 173.
[16] G. Zhang, H. Wang, Y. Yu, F. Xiong, G. Tang, W. Chen, Appl. Opt. B 76 (2003) 677.
[17] P. Poornesh, P.K. Hegde, G. Umesh, M.G. Manjunatha, K.B. Manjunatha, A.V. Adhikari, Opt. Laser Technol. 42 (2010) 230–236.
[18] F.Z. Henari, W.J. Blau, L.R. Milgrom, G. Yahioglu, D. Phillips, J.A. Lacey, Chem. Phys. Lett. 267 (1997) 229.
[19] W. Sun, C.C. Beyon, M.M. McKerns, C.M. Lawson, S. Dong, D. Wang, G.M. Gray, Proc. SPIE 16 (3798) (1999) 107.
[20] G.L. Wood, M.J. Miller, A.G. Mott, Opt. Lett. 20 (1995) 973.
[21] F.Z. Henari, J. Opt. A Pure. Appl. Opt. 3 (2001) 188.
[22] S.L. Guo, L.I. Xu, H.T. Wang, X.Z. You, N.B. Ming, Optik 114 (2003) 58–62.
[23] Ileana Rau, François Kajzar, Jérôme Luc, Bouchta Sahraoui, Georges Boudebs, J. Opt. Soc. Am. B 25 (2008) 1738–1747.
[24] R.L. Sutherland, Handbook of Nonlinear Optics, Dekker, New York, 1996.
[25] J.S. Shirk, J.R. Lindle, F.J. Bartoli, M.E. Boyle, J. Phys. Chem. 96 (1992) 5847–5852.
[26] S. Tekin, U. Kürüm, M. Durmuş, H.G. Yaglioglu, T. Nyokong, A. Elmali, Opt. Commun. 283 (2010) 4749–4753.
[27] A. Zawadzka, A. Karakas, P. Płóciennik, J. Szatkowski, Z. Łukasiak, A. Kapceoglu, Y. Ceylan, B. Sahraoui, Dyes Pigments 112 (2015) 116–126.
[28] N. Mongwaketsi, S. Khamlich, M. Pranaitis, B. Sahraoui, F. Khammar, G. Garab, R. Sparrow, M. Maaza, Mater. Chem. Phys. 134 (2012) 646–650.
[29] B. Derkowska, M. Wojdyła, R. Czaplicki, W. Bała, B. Sahraoui, Opt. Commun. 274 (2007) 206–212.
[30] Konstantinos Iliopoulos, Abdelkrim El-Ghayoury, Hasnaa El Ouazzani, Mindaugas Pranaitis, Esmah Belhadj, Emilie Ripaud, Miloud Mazari, Marc Sallé, Denis Gindre, Bouchta Sahraoui, Opt. Express 20 (2012) 25311.
[31] K. Iliopoulos, I. Guezguez, A.P. Kerasidou, A. El-Ghayoury, D. Branzea, G. Nita, N. Avarvari, H. Belmabrouk, S. Couris, B. Sahraoui, 101 (2014) 229–323.
[32] Imen Guezguez, Awatef Ayadi, Karolina Ordon, Konstantinos Iliopoulos, Diana G. Branzea, Anna Migalska-Zalas, Malgorzata Makowska-Janusik, Abdelkrim El-Ghayoury, Bouchta Sahraoui, J. Phys. Chem. C 118 (2014) 7545–7553.
[33] A. Zawadzka, P. Płóciennik, J. Strzelecki, A. Korcala, A.K. Arof, B. Sahraoui, Dyes Pigments 101 (2014) 212–220.
[34] P.G. Lacroix, Eur. J. Inorg. Chem. 2001 (2001) 339.
[35] S.D. Bella, Chem. Soc. Rev. 30 (2001) 355.
[36] C.P. Singh, K.S. Bindra, B. Jain, S.M. Oak, Opt. Commun. 245 (2005) 407.
[37] F.Z. Henari, J.Opt. A Pure Appl. Opt. 3 (2001) 188.